The High Dynamic Range Pixel Array Detector (HDR-PAD): Concept And Design

Katherine S. Shanks[1], Hugh T. Philipp[1], Joel T. Weiss[1], Julian Becker[1], Mark W. Tate[1] and Sol M. Gruner[1,2,a]

[1]*Laboratory of Atomic and Solid State Physics, Cornell University, Ithaca, NY 14853, USA*
[2]*Cornell High Energy Synchrotron Source (CHESS), Cornell University, Ithaca, NY 14853, USA*

[a]Corresponding author: smg26@cornell.edu

Abstract. Experiments at storage ring light sources as well as at next-generation light sources increasingly require detectors capable of high dynamic range operation, combining low-noise detection of single photons with large pixel well depth. XFEL sources in particular provide pulse intensities sufficiently high that a purely photon-counting approach is impractical. The High Dynamic Range Pixel Array Detector (HDR-PAD) project aims to provide a dynamic range extending from single-photon sensitivity to 10^6 photons/pixel in a single XFEL pulse while maintaining the ability to tolerate a sustained flux of 10^{11} ph/s/pixel at a storage ring source. Achieving these goals involves the development of fast pixel front-end electronics as well as, in the XFEL case, leveraging the delayed charge collection due to plasma effects in the sensor. A first prototype of essential electronic components of the HDR-PAD readout ASIC, exploring different options for the pixel front-end, has been fabricated. Here, the HDR-PAD concept and preliminary design will be described.

INTRODUCTION

As light sources become increasingly brilliant there is a need for detectors that combine the ability to tolerate high instantaneous flux with a wide dynamic range, i.e., the ability to accurately measure weak and strong signals simultaneously within any given frame. To accurately measure very weak signals, the detector read noise should be small compared to the signal generated by a single photon at the energy of interest. Here, x-ray energies around 8 keV or higher will be considered. Many photon-integrating detectors developed in recent years satisfy this constraint, with read noise that is a small fraction of an 8-keV photon, and in photon-counting detectors the read noise is automatically suppressed via in-pixel thresholding. On the high-signal end, the pixel well depth should be as large as possible. Photon-counting detectors routinely measure $> 10^6$ ph/pixel/frame; however, these detectors suffer from an inability to accurately measure photons arriving at rates exceeding $\sim 10^7$ ph/s/pixel. This rules out their use at XFELs, and can also become an issue at storage rings. Therefore, photon-integrating detectors are essential in extending wide dynamic range performance to high flux scenarios. Driven by the needs of XFEL users, several efforts are underway to produce photon-integrating detectors measuring up to $10^3 - 10^5$ ph/pixel per XFEL pulse [1, 2, 3, 4]. The High Dynamic Range Pixel Array Detector (HDR-PAD) project presented here aims to extend the dynamic range even further, measuring up to 10^6 ph/pixel per pulse and tolerating a sustained flux of 10^{11} ph/s/pixel.

THE HIGH DYNAMIC RANGE PAD

The HDR-PAD will be a hybrid pixel array detector, with a 500 µm thick high-resistivity silicon sensor bump-bonded to a separate readout ASIC. Design goals are listed in Table 1 and include targets for both XFEL and storage ring operation. Achieving the design goals will involve both optimizing the sensor operating point to account for plasma effects in the XFEL case and developing fast pixel front-end electronics.

TABLE 1: HDR-PAD design goals.

Quantity	Value
Frame rate	1 kHz (extended goal: 10 kHz)
Read noise (RMS, x-ray equivalent)	0.10 8-keV photon
Single-pulse capacity	10^6 8-keV ph/pixel/XFEL pulse
Sustained count rate	10^{11} 8-keV ph/s/pixel
Pixel size	150 μm × 150 μm

Studies of sensor plasma effects

In the XFEL case, it may be possible to leverage plasma effects, characterized in [5] for pulses of up to ~ 10^5 12-keV x-rays, to delay charge collection for pulses exceeding ~ 10^4 photons to hundreds of nanoseconds or, potentially, a microsecond, compared to the typical 10s of nanoseconds for smaller pulses. Delaying charge collection may make large pulses more tractable for the pixel front-end electronics. Studies characterizing the plasma effect using a high-powered infrared laser to simulate XFEL pulses of up to 10^6 photons are ongoing [6]. These studies aim to characterize the collection time and charge cloud spread as a function of pulse intensity, energy, focus (spot size), and sensor overbias, with the aim of finding an optimum operating point. Notably, with long charge collection delays, the lateral spread of the charge cloud may become significant, limiting the maximum acceptable delay time.

ASIC development

In the readout ASIC, each pixel will have a photon-integrating front-end combined with fast charge removal electronics to boost the pixel well capacity. This builds on the work done with the Mixed-Mode PAD (MM-PAD) [7, 8], in which charge removal is used to extend the well capacity of the photon-integrating front end to > 4×10^7 8-keV ph/pixel/frame. The MM-PAD charge removal scheme, shown in Fig. 1a, uses a gated oscillator supplying a fixed-width pulse to connect a charge removal capacitor C_{rem} to the pixel front-end input node when the front-end output reaches a fixed threshold V_{th}. The threshold is set so that charge removal is triggered when ~200 8-keV photons have been integrated. Charge removal executes in 500 ns, giving a sustained count rate limit of ~ 4×10^8 8-keV ph/s/pixel. The MM-PAD has been used successfully in a variety of experiments at storage rings, with the dynamic range proving especially useful in coherent diffractive imaging [9].

The HDR-PAD aims to extend similar performance to higher sustained flux and to allow XFEL operation. To this end, a faster version of the charge removal electronics is being developed. The repeatability of the charge removal operation is of particular concern. In the MM-PAD, the repeatability of the quantity of charge removed depends on the front-end amplifier inverting input node remaining constant at V_{ref}. This assumption will not hold true if current from the sensor arrives too quickly for the amplifier to integrate. The stability of the input node and the repeatability of charge removal will be examined carefully during testing of the HDR-PAD electronics.

The first prototype of the essential components of the HDR-PAD ASIC has been fabricated in the TSMC 0.18 μm mixed-signal process. The chips contain test structures exploring three methods of charge removal, described below.

Option 1: fast MM-PAD style charge removal

One design option, shown in Fig. 1b, uses the MM-PAD charge removal method with a few changes for increased speed. The front-end amplifier has been replaced with a class AB amplifier optimized for enhanced slew rate [10]. Adaptive gain with 2 stages has been implemented, with charge removal initiated only after the lowest-gain stage is switched in. Finally, the MM-PAD charge removal circuit is implemented with larger switches and a faster gated oscillator to allow charge removal at down to 10 ns per operation. Versions of this circuit with six different combinations of feedback capacitance and charge removal capacitance have been fabricated, to allow testing with 500 - 4000 8-keV photons per charge removal. At these charge removal rates this circuit is more promising for the high-flux storage ring case than for the high-flux XFEL case. The amplifier slew rate and charge removal control pulse width are tuneable and controlled by external biases, which will allow the determinination of the optimum operating point for the circuit. The stability of the amplifier input node, and therefore the repeatability of charge removal, in the presence of large pulses and high charge removal rates will be studied.
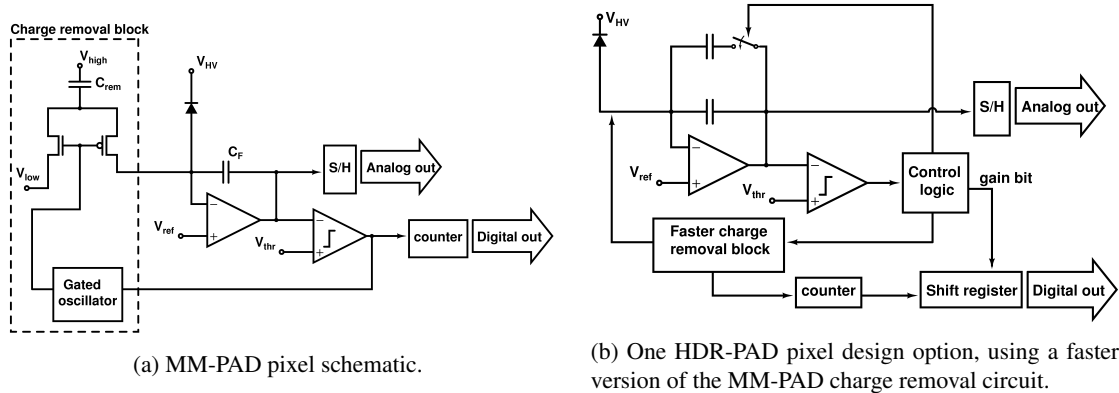
(a) MM-PAD pixel schematic.

(b) One HDR-PAD pixel design option, using a faster version of the MM-PAD charge removal circuit.
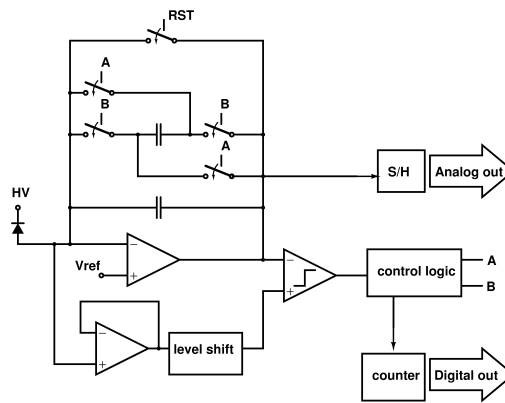
FIGURE 1: MM-PAD and HDR-PAD charge removal pixels.

FIGURE 2: Flipped-capacitor charge removal pixel schematic.

Option 2: Flipped-capacitor charge removal

The second option, shown in Fig. 2, uses a charge removal scheme inspired by the flipped-capacitor filter presented in [11]. Here, when charge removal is triggered, the polarity of one of the feedback capacitors is flipped, and stored charge on the flipped capacitor neutralizes the stored charge on the second capacitor. Although the present implementation uses two 500 fF feedback capacitors, future versions would incorporate adaptive gain with a higher-gain stage for low-intensity signals. Again, in this scheme charge removal would only operate on the lowest-gain stage.

To improve the stability of charge removal, the comparator threshold is provided by a level shifter following the front-end amplifier inverting input node, rather than being set by an external voltage. If the front-end voltage fluctuates, the comparator threshold will follow it and trigger charge removal at the appropriate time. In simulation this circuit was able to remove ~800 8-keV photons every 5 ns.

Option 3: Charge dump oscillator

The final option being tested, shown in Fig. 3a, uses a charge dump oscillator (CDO) to control charge removal. As with the flipped-capacitor circuit, adaptive gain has not been implemented in the present circuit submission but would be added in future submissions. Here, two programmable gains are included for testing purposes.

In this design, the front-end input voltage is directly monitored by a second comparator so that charge removal is triggered either when the front-end output crosses a pre-set threshold or when the front-end input starts to rise, which is an indication that the integrator is unable to keep up with the incident signal. When charge removal is triggered, the CDO is enabled and photogenerated current is shunted onto the CDO capacitor C_{CDO}, seen in Fig. 3b. When the C_{CDO} top plate voltage reaches the switching point of the adjacent inverter, a control sequence is triggered which

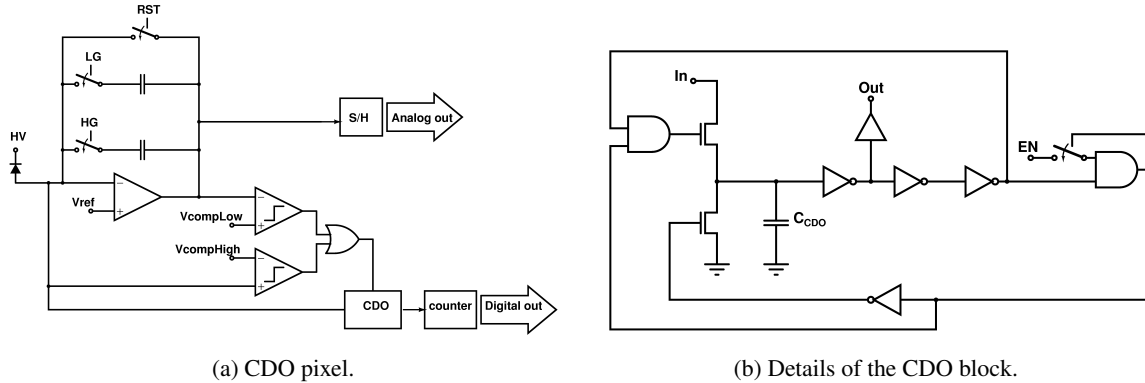(a) CDO pixel.

(b) Details of the CDO block.

FIGURE 3: Charge dump oscillator pixel schematics.

briefly shorts C_{CDO} to ground, dumping the accumulated charge. The rate at which the CDO operates tracks the rate of incoming charge, meaning that the charge removal frequency is, itself, adaptable. In simulation, removal of $\sim$ 900 8-keV photons every 2 ns was feasible. One concern is that the switching point of the CDO depends on the inverter device sizing, which may be subject to process variations.

CONCLUSION

The test structures described above have been fabricated and testing will begin in summer 2015. Testing will focus on characterizing the speed, reliability, and power consumption of the charge removal options described above. A second small-scale prototype is planned, which will be a 16×16 pixel array bonded to a silicon sensor for x-ray or laser testing and featuring the most successful pixel designs from the first prototype. Design of the second prototype will also be informed by knowledge gained from the laser studies characterizing the plasma effects in the sensor [6].

ACKNOWLEDGMENTS

REFERENCES

[1]   H. T. Philipp *et al.*, Nucl. Instr. Meth. Phys. Res., Sect. A **649**, 67–69 (2011).
[2]   B. Henrich *et al.*, Nucl. Instr. Meth. Phys. Res., Sect. A **633**, S11–S14 (2011).
[3]   M. Hart *et al.*, Nuclear Science Symposium and Medical Imaging Conference, 2012 IEEE 534 – 537 (2012).
[4]   M. Porro *et al.*, Nucl. Instr. Meth. Phys. Res., Sect. A **624**, 509 – 519 (2010).
[5]   J. Becker, "Signal development in silicon sensors used for radiation detection," Ph.D. thesis, University of Hamburg 2010.
[6]   J. T. Weiss *et al.*, SRI 2015 Conference Proceedings (2015).
[7]   D. Schuette, "A mixed analog and digital pixel array detector for synchrotron x-ray imaging," Ph.D. thesis, Cornell University 2008.
[8]   M. Tate *et al.*, Journal of Physics: Conference Series **425**, p. 062004 (2013).
[9]   K. Giewekemeyer *et al.*, J. Synchrotron Radiation **21**, 1167–1174 (2014).
[10]   A. J. López-Martín *et al.*, IEEE Journal of Solid-State Circuits **40** (2005).
[11]   L. Ratti *et al.*, Nucl. Instr. Meth. Phys. Res., Sect. A (2015).